Phase Transitions

Deutsche Ausgabe: DOI: 10.1002/ange.201501344
Internationale Ausgabe: DOI: 10.1002/anie.201501344

A Chemically Triggered and Thermally Switched Dielectric Constant Transition in a Metal Cyanide Based Crystal**

Chao Shi, Xi Zhang, Ying Cai, Ye-Feng Yao, and Wen Zhang**

Abstract: *A dielectric constant transition is chemically triggered and thermally switched in $(HPy)_2[Na(H_2O)Co(CN)_6]$ (**2**, HPy = pyridinium cation) by single-crystal-to-single-crystal transformation and structural phase transition, respectively. Upon dehydration, $(HPy)_2[Na(H_2O)_2Co(CN)_6]$ (**1**) transforms to its semi-hydrated form **2**, accompanying a transition from a low-dielectric state to a high-dielectric state, and vice versa. This dielectric switch is also realized by a structural phase transition in **2** that occurs between room- and low-temperature phases, and which corresponds to high- and low-dielectric states, respectively. The switching property is due to the variation in the environment surrounding the HPy cation, that is, the hydrogen-bonding interactions and the crystal packing, which exert predominant influences on the dynamics of the cations that transit between the static and motional states.*

Stimuli-responsive materials are those that can change their physical and/or chemical properties to enable responses to external stimuli such as temperature, light, pressure, electric and magnetic fields, radiation, and specific chemicals (for example, use of solvents and different changes in pH value).[1–5] Some properties can be switched between at least two states, which can thus be used in sensors, switches, and memory devices. Typical examples are spin-crossover (SCO) compounds, in which the magnetic state can be switched between low- and high-spin states because of spin pairing and unpairing (for example, low- and high-spin Fe^{II} ion: $t_{2g}^6e_g^0$ $(S=0)\leftrightarrow t_{2g}^4e_g^2$ $(S=2)$).[5,6] As an electric counterpart, a switchable dielectric constant (SDC) shows switching behaviors analogous to the SCO.[7,8] The dielectric constant or electric permittivity ε' ($\varepsilon=\varepsilon'-i\varepsilon''$) reflects the degree of electric polarizability of a material and is microscopically associated with dipolar motions such as molecular rotations if they exist.[9] For molecular crystals, the dielectric transition between low- and high-dielectric states is established by the reorientation transformation of polar components between static (that is, frozen) and dynamic (motional) phases, which are often accompanied by a structural phase transition (PT).[10] This is an amphidynamic feature, that is, both static and dynamic components assembled together in a crystal,[11] which link the SDC compounds closely to crystalline molecular rotors that exhibit diverse properties.[12–20]

Among the various stimuli, temperature is the most frequently used trigger. In contrast, fewer results have been reported on responsive materials that are triggered by stimuli besides temperature.[3,5] In the case of SDCs, the multi-switchable property would greatly expand understanding and potential applications of SDC materials. Herein, we report a crystalline compound showing a SDC that is dually triggered by chemical and thermal stimuli. In the crystal $(HPy)_2[Na(H_2O)_2Co(CN)_6]$ (**1**, HPy = pyridinium cation), the HPy cation is static, and thus the compound remains in a low-dielectric state. Upon dehydration, **1** transforms to its semi-hydrated form $(HPy)_2[Na(H_2O)Co(CN)_6]$ (**2**), in which the HPy cation transforms to a dynamic state, resulting in a high-dielectric state. This process is a chemically triggered SDC. Furthermore, the HPy cation in **2** undergoes a dynamic change between the static and motional states at about 230 K. The motion of the HPy cation is switched by temperature, which results in a transition between low and high dielectric states.

Compound **1** was obtained as block crystals by evaporation of an aqueous solution containing pyridinium chloride and $Na_3[Co(CN)_6]$. Its structure was first solved at 293 K. Compound **1** crystallizes in the orthorhombic space group *Cmca* with $a=10.980(2)$ Å, $b=16.143(3)$ Å, and $c=11.159(2)$ Å (Supporting Information, Tables S1–S3). The anionic $[Na(H_2O)_2Co(CN)_6]$ part shows a two-dimensional grid-like structure in the *b* plane (Figure 1a; Supporting Information, Figure S1). Each $[Co(CN)_6]$ unit connects with four Na ions through four CN groups, leaving the remaining two *trans* CN groups as terminal ligands. The Na ion is bound to four bridging CN groups (Na1−N2 = 2.435 Å and Na1-N2-C2 = 180.0° along the *a* direction; Na1−N3 = 2.604 Å and Na1-N3-C3 = 162.9° along the *c* direction) and two terminal water molecules (Na1−O1 = 2.476 Å), showing a highly distorted octahedral coordination geometry (N3-Na1-O1 = 69.3° and 110.7°). Therefore, the grid plane shows a slight wave-like or rippled surface pattern. Neighboring grids stack along the *b* direction with the shortest Co···Na distance of 8.072 Å, which are linked to each other by hydrogen bonds between the terminal CN groups and water molecules (N1···O1 = 2.757 Å). Consequently, supramolecular cages form between the grids, in which the HPy cation resides and is fixed through a hydrogen bond between the N atom of the ring and the

[*] C. Shi, Y. Cai, Prof. W. Zhang
Ordered Matter Science Research Center
Southeast University, Nanjing 211189, Jiangsu (China)
E-mail: zhangwen@seu.edu.cn
X. Zhang, Prof. Y.-F. Yao
Department of Physics & Shanghai Key Laboratory of Magnetic Resonance, East China Normal University
North Zhongshan Road 3663, Shanghai 200062 (China)
E-mail: yfyao@phy.ecnu.edu.cn

[**] This work was financially supported by the NSFC (Grant No. 21225102 and 21174039). We thank beamline BL14B (Shanghai Synchrotron Radiation Facility) for providing the beam time.
Supporting information for this article is available on the WWW under http://dx.doi.org/10.1002/anie.201501344.

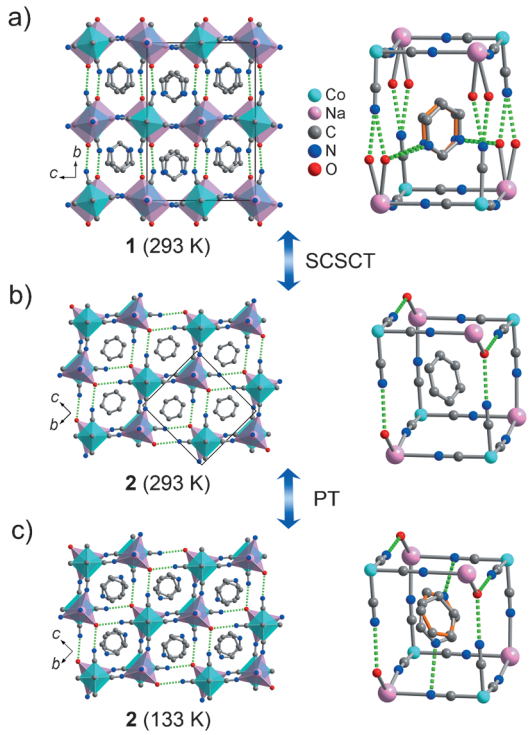

Figure 1. Changes in the crystal packing (left) and supramolecular cage-like environment around the HPy cation (right) of a) **1** at 293 K, b) **2** at 293 K, and c) **2** at 133 K upon single-crystal-to-single-crystal transformation and structural phase transition. Green dotted lines represent hydrogen bonds. Hydrogen atoms are omitted for clarity. The two-site disordered HPy cations in (a) and (c) are distinguished by different bond colors.

water molecule (N···O = 2.872 Å). Two-site disorders are found in the HPy cation and water molecule.

The crystals of **1** gradually effloresce in dry air at room temperature (Supporting Information, Figure S2). Thermal gravimetric analysis (TGA) shows that it loses two water molecules per formula unit in two steps at around 320 K and 420 K, respectively, followed by decomposition at about 446 K (Supporting Information, Figure S3). Between the two steps, **1** loses half of its coordinated water molecules and retains stability in its semi-hydrated form **2** by a single-crystal-to-single-crystal transformation (SCSCT).

At 293 K, **2** still crystallizes in the orthorhombic system but with the space group *Pmmn*. Compared with **1**, the corresponding cell parameters also markedly change with $a =$ 11.151(10) Å, $b = 8.821(8)$ Å, and $c = 9.684(8)$ Å. In the structure, the $[Co(CN)_6]$ component is unchanged owing to its structural rigidity. In contrast, the Na ion undergoes a striking coordination change from a highly distorted octahedral geometry (N_4O_2) to a slightly distorted trigonal-bipyramidal geometry (N_4O) (Figure 1 b). The Na–N lengths are in the range 2.483–2.539 Å and the Na–O bond length is decreased to 2.364 Å. The $[Co(CN)_6]$ unit still connects with four Na ions through four CN groups, but leaves untouched the remaining two *cis* CN groups as terminal ligands. These two large coordination changes result in a zigzag-shaped surface of the CoNa grid plane with a dihedral angle of 106.1°. Neighboring grids are very well connected by N···HO hydrogen bonds (2.759 Å) between the terminal CN groups and the water molecules. The hydrogen-bonded water molecules contribute to the high thermal stability of **2**, which loses the coordinated water above 420 K. The resulting irregular supramolecular cage is heavily distorted because the Na–O bonds are not aligned with the Co–C≡N edges. Although it is still trapped in the newly formed cage, the HPy cation undergoes a high disorder with indistinguishable C and N atoms in the six-numbered ring, which is totally different from the state seen for **1**.

It is notable that both **1** and **2** have a highly-distorted double perovskite-type structure formulated as $A_2[B'B''(CN)_6]$ if the water molecules are ignored.[7] The structural transformation between the two compounds is proposed as a relative displacement in opposite directions of the neighboring Co–C≡N–Na chains that extend along the *a* axis (Supporting Information, Figure S4). These alterations cause about +1.6 %, −19.2 %, and +17.4 % of the changes seen in the corresponding axes (by reference to **1**) of the crystal.[20,21] The driving force is a change in the coordination geometry of the Na center that plays a key role in the stability of the hydrogen network in the crystal lattice. This structural rearrangement strikingly alters the environment around the HPY cation, which results in different dynamic states of the cations that are found in **1** and **2**.

When **2** is cooled to 133 K, the space group is still *Pmmn* and the cell parameters show inflections around the transition point (Supporting Information, Figure S5). The most striking change in the structure is the HPy cation. The C and N atoms in the ring are totally distinguishable (Figure 1 c). However, the cation shows a static disorder over two sites with a dihedral angle of 9.84° in two orientations. The ring is anchored in the cage by a hydrogen bond between the terminal CN group and the N atom of the HPy (NH···N = 2.984 Å). This dynamic change of the HPY cation is accompanied by the structural PT in **2**.

The whole process of the SCSCT from **1** to **2** and the structural PT in **2** was further demonstrated by variable-temperature (VT) powder X-ray diffraction (PXRD) and differential scanning calorimetry (DSC) measurements (Figure 2). Upon heating, the PXRD pattern of **1** at 353 K is completely different from the one found at 298 K, which indicates transformation to the semi-hydrated form **2**. It also completely recovers to the hydrated form **1** in two days following exposure to water vapor at room temperature. The type I isotherm of **1** reveals that the adsorption and desorption of water vapor at 298 K is not completed immediately (Supporting Information, Figure S7). These results demonstrate the reversibility of the SCSCT between **1** and **2**. Moreover, DSC analysis shows that the semi-dehydration from **1** to **2** occurs at approximately 330 K with a strong endothermic peak. Upon further cooling–warming cycles, the water-loss peak disappears and a pair of peaks appears in the low-temperature region at around 228 K, which verifies the occurrence of the reversible solid-state PT in **2**. The measured enthalpy change and corresponding calculated entropy change of the PT are 0.275 kJ mol^{-1} and 1.20 J mol^{-1} K^{-1}, respectively.

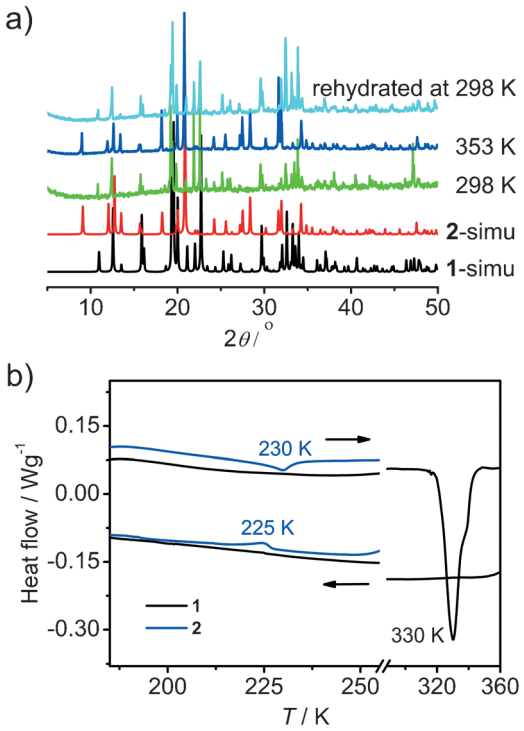

Figure 2. a) Variable-temperature PXRD patterns of **1** upon heating and hydration at 298 K, together with the simulated patterns of **1** and **2** from single-crystal X-ray diffraction data. b) DSC curves of **1** as measured in two cooling-heating cycles.

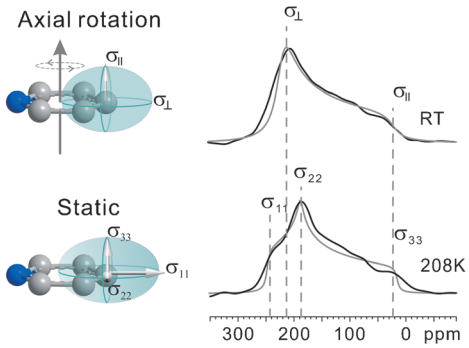

Figure 3. ^{13}C CSA patterns of the *p*-C of HPy cation of **2** below and above the phase transition point. The gray lines are the simulated ^{13}C CSA patterns to fit the experimental patterns (the black lines) that are acquired at room temperature and at 208 K, respectively.

To understand the local reorientation process of HPy cations, a preliminarily solid-state NMR study was applied to **2**. Figure 3 shows the ^{13}C chemical shift anisotropy (CSA) powder patterns of the *para*-C (*p*-C) of HPy cation of **2** below and above the phase transition point, which are extracted from the 2D SUPER spectra (Supporting Information, Figure S8).[22a] Intriguingly, the pattern of *p*-C shows a typical asymmetric tensorial powder lineshape below the transition point, whereas above the transition point the pattern shows typical features of an axially symmetric tensor with $\sigma_\perp$ close to $(\sigma_{11}+\sigma_{22})/2$ and $\sigma_\parallel$ close to σ_{33}. In the literature, the ^{13}C CSA tensor orientation of *p*-C of a static HPy in the molecular frame has been measured, that is, σ_{11} and σ_{22} are located in the HPy ring plane and σ_{33} is perpendicular to the ring plane.[22b] The tensor features of the *p*-C above the transition point thus strongly indicate that the HPy cations likely undergo a restricted anisotropic motion close to an axial in-plane rotation, which could average σ_{11} and σ_{22} to $\sigma_\perp$ and retain an unaltered σ_{33}. Furthermore, the above single-crystal structures have shown only a small change of the position of the HPy cation in the supramolecular cage below and above the transition point. This indicates that the rotation axis of the HPy cation is in all likelihood perpendicular to the plane of the HPy ring. Under this rotational geometry, the rotation of the HPy cations might have induced oscillation of the dipole moment, which would result in a switchable dielectric constant in **2** as discussed below. An NMR study on the correlation between the dynamics of the HPy cation and the switchable dielectric constant of **2** is currently under way.

Dielectric constant measurements were performed on the powdered samples **1** and **2** in the range 120–350 K and 1–1000 kHz (Figure 4; Supporting Information, Figure S9). For

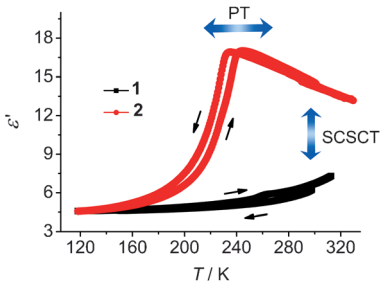

Figure 4. Temperature dependence of the real part of the dielectric constant on the powdered samples of **1** and **2** at 1 MHz.

1, the ε' keeps stable below 250 K with a value of about 5, which corresponds to a low-dielectric state. It gradually increases above 273 K, which is due to gradual water activation in the crystal lattice. For **2**, the high-dielectric state is retained at room temperature. Upon cooling, the ε' value increases to reach a peak value of about 17 at 230 K. This trend reflects the competition between orientational polarization upon electric field and random thermal motion of the HPy cations. A rapid drop is then followed to a value of about 5 at 140 K, which corresponds to a transition to the low-dielectric state. These dielectric changes are associated with the static-motional transitions of the polar HPy cations in the crystal. It is thought that the polar motion is much faster than 1 MHz because there is no evidence of frequency dependence in the measured frequency range. A pretransitional effect in **2** is also observed in the temperature range 170–220 K, which is shown as a gradual increase in ε' below the transition point of 230 K. This is supposed to be caused by a partial activation of the polar HPy cation.[7b]

As mentioned above, the SDC arises from the contribution of molecular dipolar reorientation. However, the relationship among dielectric constant, dipole moment and temperature in condensed matter is not simple due to complicated intermolecular interactions.[23] Considering the fact that the dipole moment of the HPy cation is strictly confined in the rigid ring plane and the motional HPy cations

are well-segregated by the metal-cyanide framework in the crystal lattice, the assembly of the cations can be simplified as a dipolar liquid model. Therefore, the following Kirkwood–Fröhlich equation can be used to fit the experimental data of **2** in the high-dielectric state:

$$\frac{(\varepsilon' - \varepsilon_\infty)(2\varepsilon' + \varepsilon_\infty)}{\varepsilon'(\varepsilon_\infty + 2)^2} = \frac{N\mu^2}{9\varepsilon_0 k_B T} \cdot g_K$$

where the Kirkwood factor g_K is used to measure the interactions among the dipoles (Supporting Information, Figure S10).[9,24] The calculated g_K shows a slight temperature dependence in the high-dielectric state of **2** with values of 1.08 at 323 K and 1.11 at 263 K, which indicates the existence of weak intermolecular interactions. This result is consistent with the observations in the crystal structures (Supporting Information, Figure S5). It should be noted that ferroelectric or anti-ferroelectric behaviors would be generated if the dipole carriers are strongly coupled.[8e,12]

Relationship between the structure and the SDC is thus established. In **1**, the HPy cation is fixed in the supramolecular cage by a relatively strong NH···O hydrogen bond. It undergoes a static disorder over two sites with equivalent occupancies that does not contribute to the dielectric constant. Thus **1** remains in the low-dielectric state until it undergoes dehydration to transform to **2** where the HPy cation shows a dynamic disorder that contributes to the dielectric constant, which corresponds to the high-dielectric state. The disordered state is ascribed to the strikingly weakened NH···N hydrogen bonds that are located between the HPy cation and the new supramolecular cage that make the motion possible. When the temperature decreases to a point where the strength of the NH···N hydrogen bond overwhelms thermal agitation, the HPy cation transforms to a static disorder, which corresponds to a structural PT. This change leads to the low-dielectric state of **2**.

In conclusion, the chemically triggered and thermally switched dielectric constant is realized in $(HPy)_2[Na(H_2O)Co(CN)_6]$ (HPy = pyridinium cation) by single-crystal-to-single-crystal transformation and structural phase transition, respectively. The dual switching properties rely on the variation of the environment around the HPy cation, that is, hydrogen-bonding interactions and crystal packing, which exert predominant influence on the dynamics of the cation that transits between the static and motional states.

Keywords: cyanide · phase transitions · pyridinium · single-crystal-to-single-crystal transformations · switchable dielectric constant

How to cite: *Angew. Chem. Int. Ed.* **2015**, *54*, 6206–6210
Angew. Chem. **2015**, *127*, 6304–6308

[1] *Handbook of Stimuli-Responsive Materials* (Ed.: M. W. Urban), Wiley-VCH, Weinheim, **2011**.
[2] M. A. C. Stuart, W. T. S. Huck, J. Genzer, M. Müller, C. Ober, M. Stamm, G. B. Sukhorukov, I. Szleifer, V. V. Tsukruk, M. Urban, F. Winnik, S. Zauscher, I. Luzinov, S. Minko, *Nat. Mater.* **2010**, *9*, 101.
[3] S. Horike, S. Shimomura, S. Kitagawa, *Nat. Chem.* **2009**, *1*, 695.
[4] a) S. Horiuchi, Y. Tokura, *Nat. Mater.* **2008**, *7*, 357; b) W. Zhang, R. G. Xiong, *Chem. Rev.* **2012**, *112*, 1163.
[5] O. Sato, J. Tao, Y.-Z. Zhang, *Angew. Chem. Int. Ed.* **2007**, *46*, 2152; *Angew. Chem.* **2007**, *119*, 2200.
[6] a) O. Kahn, *Molecular Magnetism*, VCH, New York, **1993**; b) P. Gütlich, H. A. Goodwin, *Top. Curr. Chem.* **2004**, 233.
[7] a) W. Zhang, Y. Cai, R.-G. Xiong, H. Yoshikawa, K. Awaga, *Angew. Chem. Int. Ed.* **2010**, *49*, 6608; *Angew. Chem.* **2010**, *122*, 6758; b) W. Zhang, H.-Y. Ye, R. Graf, H. W. Spiess, Y.-F. Yao, R.-Q. Zhu, R.-G. Xiong, *J. Am. Chem. Soc.* **2013**, *135*, 5230; c) X. Zhang, X.-D. Shao, S.-C. Li, Y. Cai, Y.-F. Yao, R.-G. Xiong, W. Zhang, *Chem. Commun.* **2015**, *51*, 4568.
[8] a) P. Jain, N. S. Dalal, B. H. Toby, H. W. Kroto, A. K. Cheetham, *J. Am. Chem. Soc.* **2008**, *130*, 10450; b) X.-H. Zhao, X.-C. Huang, S.-L. Zhang, D. Shao, H.-Y. Wei, X.-Y. Wang, *J. Am. Chem. Soc.* **2013**, *135*, 16006; c) C.-M. Ji, Z.-H. Sun, S.-Q. Zhang, T.-L. Chen, P. Zhou, J.-H. Luo, *J. Mater. Chem. C* **2014**, *2*, 567; d) Z.-Y. Du, T.-T. Xu, B. Huang, Y.-J. Su, W. Xue, C.-T. He, W.-X. Zhang, X.-M. Chen, *Angew. Chem. Int. Ed.* **2015**, *54*, 914; *Angew. Chem.* **2015**, *127*, 928; e) R. Shang, Z.-M. Wang, S. Gao, *Angew. Chem. Int. Ed.* **2015**, *54*, 2534; *Angew. Chem.* **2015**, *127*, 2564.
[9] H. Fröhlich, *Theory of dielectrics, 2nd ed.*, Oxford University Press, Oxford, **1965**.
[10] Y. A. Izyumov, V. N. Syromyatnikov, *Phase Transitions and Crystal Symmetry*, Kluwer, Dordrecht, **1990**.
[11] a) M. A. Garcia-Garibay, *Proc. Natl. Acad. Sci. USA* **2005**, *102*, 10771; b) S. D. Karlen, M. A. Garcia-Garibay, *Top. Curr. Chem.* **2005**, *262*, 179; c) S. D. Karlen, H. Reyes, R. E. Taylor, S. I. Khan, M. F. Hawthorne, M. A. Garcia-Garibay, *Proc. Natl. Acad. Sci. USA* **2010**, *107*, 14973.
[12] a) T. Akutagawa, H. Koshinaka, D. Sato, S. Takeda, S. Noro, H. Takahashi, R. Kumai, Y. Tokura, T. Nakamura, *Nat. Mater.* **2009**, *8*, 342; b) P. Jain, V. Ramachandran, R. J. Clark, H. D. Zhou, B. H. Toby, N. S. Dalal, H. W. Kroto, A. K. Cheetham, *J. Am. Chem. Soc.* **2009**, *131*, 13625; c) D.-W. Fu, W. Zhang, H.-L. Cai, Y. Zhang, J.-Z. Ge, R.-G. Xiong, S. D. Huang, T. Nakamura, *Angew. Chem. Int. Ed.* **2011**, *50*, 11947; *Angew. Chem.* **2011**, *123*, 12153; d) G.-C. Xu, W. Zhang, X.-M. Ma, Y.-H. Chen, L. Zhang, H.-L. Cai, Z.-M. Wang, R.-G. Xiong, S. Gao, *J. Am. Chem. Soc.* **2011**, *133*, 14948; e) Y. Zhang, W. Zhang, S.-H. Li, Q. Ye, H.-L. Cai, F. Deng, R.-G. Xiong, S. D. Huang, *J. Am. Chem. Soc.* **2012**, *134*, 11044.
[13] M. Horie, Y. Suzaki, D. Hashizume, T. Abe, T. Wu, T. Sassa, T. Hosokai, K. Osakada, *J. Am. Chem. Soc.* **2012**, *134*, 17932.
[14] J. A. Rodríguez-Velamazán, M. A. González, J. A. Real, M. Castro, M. C. Muñoz, A. B. Gaspar, R. Ohtani, M. Ohba, K. Yoneda, Y. Hijikata, N. Yanai, M. Mizuno, H. Ando, S. Kitagawa, *J. Am. Chem. Soc.* **2012**, *134*, 5083.
[15] C. Lemouchi, K. Iliopoulos, L. Zorina, S. Simonov, P. Wzietek, T. Cauchy, A. Rodríguez-Fortea, E. Canadell, J. Kaleta, J. Michl, D. Gindre, M. Chrysos, P. Batail, *J. Am. Chem. Soc.* **2013**, *135*, 9366.
[16] W. Setaka, K. Yamaguchi, *J. Am. Chem. Soc.* **2013**, *135*, 14560.
[17] E. Coronado, M. Giménez-Marqués, G. M. Espallargas, F. Rey, I. J. Vitórica-Yrezábal, *J. Am. Chem. Soc.* **2013**, *135*, 15986.
[18] C. R. Murdock, N. W. McNutt, D. J. Keffer, D. M. Jenkins, *J. Am. Chem. Soc.* **2014**, *136*, 671.
[19] A. Comotti, S. Bracco, A. Yamamoto, M. Beretta, T. Hirukawa, N. Tohnai, M. Miyata, P. Sozzani, *J. Am. Chem. Soc.* **2014**, *136*, 618.
[20] Z.-S. Yao, M. Mito, T. Kamachi, Y. Shiota, K. Yoshizawa, N. Azuma, Y. Miyazaki, K. Takahashi, K. Zhang, T. Nakanishi, S. Kang, S. Kanegawa, O. Sato, *Nat. Chem.* **2014**, *6*, 1079.
[21] a) T. K. Maji, K. Uemura, H.-C. Chang, R. Matsuda, S. Kitagawa, *Angew. Chem. Int. Ed.* **2004**, *43*, 3269; *Angew. Chem.* **2004**, *116*, 3331; b) C. L. Chen, A. M. Goforth, M. D. Smith, C.-Y. Su, H. C. zur Loye, *Angew. Chem. Int. Ed.* **2005**, *44*, 6673; *Angew. Chem.* **2005**, *117*, 6831; c) C. Serre, C. Mellot-

Draznieks, S. Surble, N. Audebrand, Y. Filinchuk, G. Férey, *Science* **2007**, *315*, 1828; d) B. Wei, R. Shang, X. Zhang, X.-D. Shao, Y.-F. Yao, Z.-M. Wang, R.-G. Xiong, W. Zhang, *Chem. Eur. J.* **2014**, *20*, 8269.

[22] a) S. F. Liu, J. D. Mao, K. Schmidt-Rohr, *J. Magn. Reson.* **2002**, *155*, 15; b) P. Parhami, B. M. Fung, *J. Am. Chem. Soc.* **1985**, *107*, 7304.

[23] A. K. Jonscher, *Dielectric Relaxation in Solids*, Chelsea Dielectrics Press, London, **1983**.

[24] J. G. Kirkwood, *J. Chem. Phys.* **1939**, *7*, 911.

Received: February 11, 2015
Published online: April 1, 2015

